Supporting Information

A quasi-solid-state self-healing flexible zinc-ion battery using dual-crosslinked hybrid hydrogel as electrolyte and Prussian blue analogue as cathode material

Jiawei Long[a], Tianli Han[a], Xirong Lin[b], Yajun Zhu[a,c], Jinyun Liu*[,a], Junjie Niu*[,d]

[a] Key Laboratory of Functional Molecular Solids, Ministry of Education, College of Chemistry and Materials Science, Anhui Normal University, Wuhu, Anhui 241002, PR China. E-mail: jyliu@ahnu.edu.cn

[b] National Key Laboratory of Science and Technology on Micro/Nano Fabrication, Department of Micro/Nano-electronics, Shanghai Jiao Tong University, Shanghai 200240, PR China

[c] Institute of Energy, Hefei Comprehensive National Science Center, Hefei, Anhui 230031, PR China

[d] Department of Materials Science and Engineering, University of Wisconsin-Milwaukee, Milwaukee, 53211, Wisconsin, USA. E-mail: niu@uwm.edu

1. Synthesis of cobalt hexacyanoferrate NPs

All the chemicals were commercially available and used without further purification. Cobalt hexacyanoferrate nanoparticles were synthesized via a coprecipitation method. In a typical experiment, 5.0 mmol $Co(CH_3COO)_2 \cdot 4H_2O$ (AR, Aladdin) was dissolved in 50 mL deionized (DI) water under magnetic stirring (HJ-4B, Yidu) (denoted as solution A). Another 5.0 mmol $K_3Fe(CN)_6$ (AR, Aladdin) and 5.0 g polyvinyl pyrrolidone (PVP, K30, AR, Aladdin) were dissolved in 150 mL DI water to form a transparent solution (denoted as solution B). Subsequently, the solution A was dropwise added into the solution B. After stirring for 1 h, the suspension was stored at room temperature for 24 h. The received dark purple precipitate was collected by centrifugation (12000 rpm for 20 min). Then the sample was washed several times with DI water and ethanol, and dried at 80 °C in an oven (DHG-9050A, Jinghong) for 12 h.

2. Preparation of the hybrid hydrogel electrolyte

The hydrogel electrolyte was prepared via *in-situ* photoinitiated radical polymerization. Typically, certain mass of acrylamide (AM, AR, Aladdin), 0.5 g PVA (Mw=13000~23000, 87~89% hydrolyzed, AR, Aladdin) and 0.5 mg N,N'-methylenebisacrylamide (MBA, AR, Aladdin) were dissolved in 5.0 mL 1.0 M $Zn(CH_3COO)_2$ (AR, Aladdin) liquid electrolyte to form a mixture solution under magnetic

stirring at 85 °C. After cooling down to room temperature, 10.0 μL 2-hydroxy-2-methylpropiophenone (HMPP, 97%, AR, Aladdin) was dispersed in the above solution before poured it into a Petri dish. The free-radical polymerization was conducted by ultraviolet (UV) irradiation (HY-UV0003, Lightwells) for 120 s under ice bath. The sample with a composition of 0.5 g PVA + 0.5 mg MBA + 2.0 g AM was used as the optimized hydrogel electrolyte.

3. Characterizations

The morphology, structure and composition of the sample were investigated on a scanning electron microscopy (SEM, Hitachi S8100, operated at 5 kV), a transmission electron microscopy (TEM, Hitachi HT7700) and a high-resolution transmission electron microscopy (HRTEM, FEI TalosF200x), and X-ray diffraction (XRD, Rigaku SmartLab) with the Cu Kα of 1.5418 Å, respectively. X-ray photoelectron spectroscopy (XPS, Escalab 250Xi) was used to analyze the elemental state. All the spectra were calibrated by the binding energy of C1s at 284.8 eV. Brunauer-Emmett-Teller measurements (BET, Nova 2000E) was used to determine the surface area and pore distribution. Thermogravimetry analysis (TGA, TA5500) was employed to measure the mass of K. The obtained hydrogel was immersed in liquid nitrogen then freeze-dried for 48 h for FTIR (INVENIO IR-21) and Raman (inVia, Renishaw) tests. The functional groups of the sample were studied by using Fourier transform infrared (FT-IR) spectroscopy (INVENIO IR-21) and Raman spectrometry (inVia, Renishaw).

4. Electrochemical property and battery performance tests

Electrochemical impedance spectroscopy (EIS), linear scan voltammetry (LSV) and cyclic voltammetry (CV) were carried out on an electrochemical workstation (CHI-660e, Chenhua). The assembled Zn||Zn symmetric and Zn||Cu asymmetric cells were measured on a battery tester (CT-4008, Neware). LSV measurement was conducted at a scanning rate of 5 mV s^{-1} by using three electrodes system where stainless-steel foils (SS, 1 cm^2) were respectively used as working and counter electrodes and Ag/AgCl (1.0 M KCl) was used as reference electrode.

The ionic conductivity of the electrolyte was evaluated in a stainless-steel (SS)||electrolyte||SS symmetric cell. All the tests were carried out on the electrochemical station by A.C. impedance method with a frequency range from 1.0 to 10^5 Hz. The data was calculated based on the equation[1,2]:

$$\sigma = \frac{L}{R * A}$$

where σ stands for the ionic conductivity, S cm^{-1}, R is the resistance (Ω), A is the contact area of the electrolyte (here it is 1.0 cm^2), and L (cm) is the distance between SS foils, respectively.

The stability of the electrolyte was also investigated by Zn||Zn symmetric batteries, in which two metallic Zn foils (≈10 μm) were used as cathode and anode. The cell was tested under different current densities and areal capacities. The Coulombic efficiency (CE) was performed using Cu foil (≈10 μm) and Zn foils as cathode and anode, respectively. The cutoff voltage of Zn||Cu half-batteries during charging were set to 1.0 V.

For the battery assembly, cobalt hexacyanoferrate NPs, carbon black (EL, Aladdin) and poly(vinylidene fluoride) (PVDF, AR, Aladdin) were mixed with a mass ratio of 9:0.5:0.5 and dispersed in N-methyl-2-pyrrolidone (NMP, EL, Aladdin) solvent under magnetic stirring. The formed slurry was dropped on a carbon cloth (CC, CeTech, WOS1002) and dried at 80 °C in a vacuum oven (DZF-6020, Jinghong). The mass loading of active material was controlled to be 5.0~7.8 mg cm^{-2}. As a comparison, the slurry was also casted on graphite paper (Guanzhi, Shandong) and dried under the same condition. The obtained cathode electrode with a mass loading of 0.9~2.3 mg cm^{-2} was cut into a circle disc with a diameter of 12.0 mm.

The electroplating solution was prepared by dissolving 10.0 g anhydrous $Zn(CH_3COO)_2$ (AR, Aladdin) in a mixture solution of 30.0 mL DI water and 20.0 mL dimethyl sulfoxide (DMSO, AR, Aladdin). Then the Zn/CC electrode was prepared by using amperometric *i-t* method at –1.8 V for 45 min. The mass loading of Zn on carbon cloth was 9.7~12.4 mg cm^{-2}.

The quasi-solid-state pouch cell was assembled by using cobalt hexacyanoferrate NPs/CC (2.5 × 2.5 cm^2), Zn/CC (2.5 × 2.5 cm^2) and hybrid hydrogel (2.6 × 2.6× 0.4 cm^3) as cathode material, anode material and electrolyte, respectively. The sandwiched-like battery was sealed with aluminum laminated film (ALF) on a vacuum sealing machine (MSK-140, Kejing). As comparisons, pure PAM hydrogel electrolyte was parepared by polymerizing 2.5 g AM in liquid electrolyte. The quasi-solid-state AZIB with pure PAM hydrogel electrolyte was assembled *via* same process. Besides, the CR2032 coin cell battery with liquid electrolyte soaked glass fibers as electrolyte was also assembled.

The capacitive and diffusion-controlled behavior was evaluated in terms of the equation: $i=av^b$ and $\log(i) = b\log(v) + \log(a)$, where i (mA) and v (mV s^{-1}) stand for the current and scanning rate, while a and b present the changeable parameters, respectively[3,4]. The pseudocapacitive contribution ratios at various sweep rates were estimated according to the equation: $i(V) = k_1v + k_2v^{1/2}$, where k_1v and $k_2v^{1/2}$

stand for non-Faradaic (capacitive behavior) and Faradaic (diffusion-controlled process) process[5]. The values of k_1 and k_2 were calculated by transforming the equation to $i(V)/v^{1/2} = k_1 v^{1/2} + k_2$ and plotted by $i(V)/v^{1/2}$ versus $v^{1/2}$.

Galvanostatic intermittent titration technique (GITT) measurements were conducted at 100 mA g^{-1} on a battery tester (CT-4008, Neware).

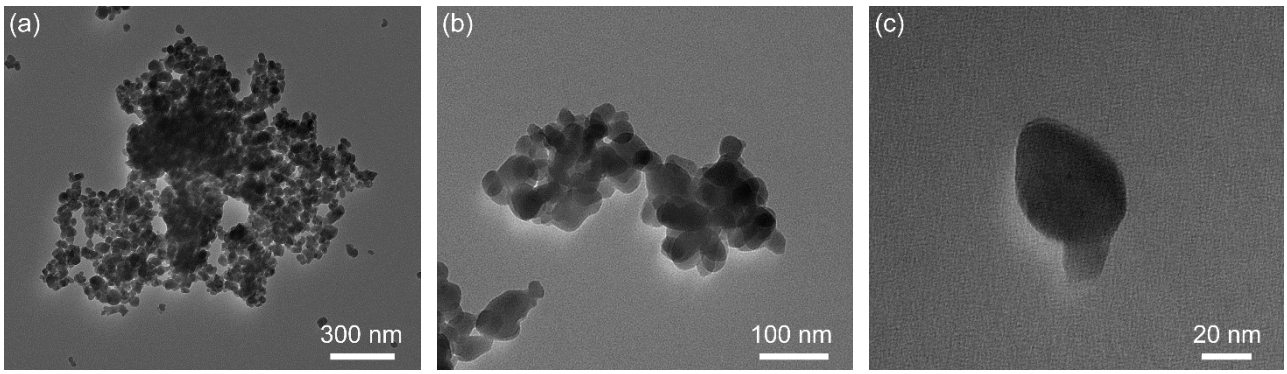

Figure S1. TEM images of the as-received cobalt hexacyanoferrate.

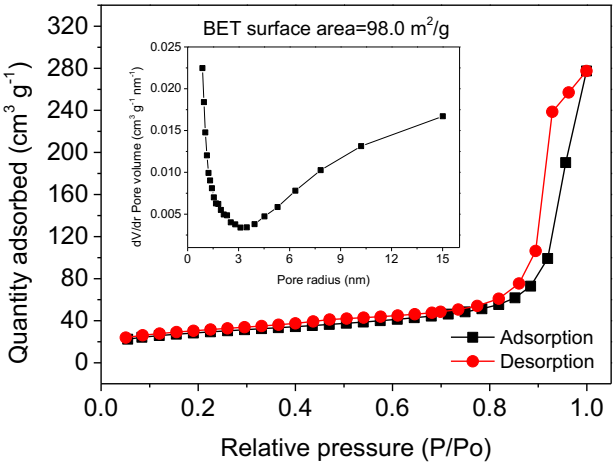

Figure S2. N_2 adsorption/desorption isotherms of the cobalt hexacyanoferrate NPs. The inset shows the pore size distribution.

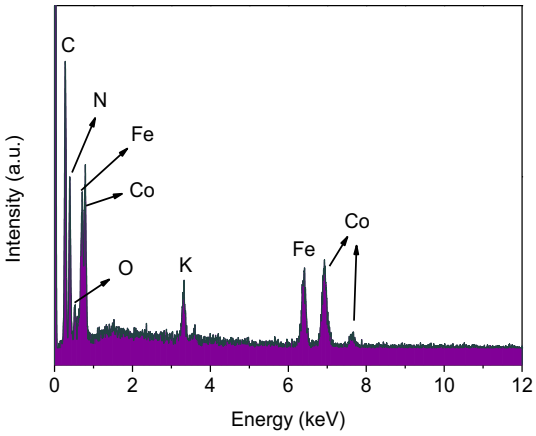

Figure S3. EDS spectrum of the cobalt hexacyanoferrate NPs.

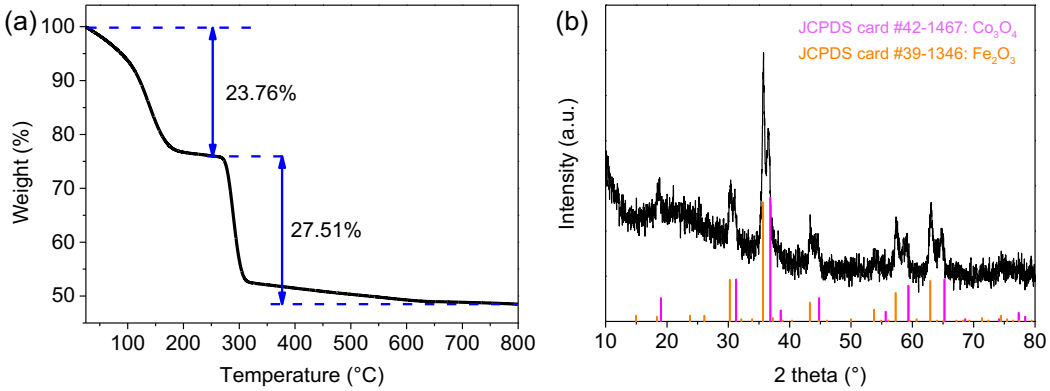

Figure S4. (a) TGA curve of the cobalt hexacyanoferrate and (b) XRD pattern of the sample after TGA test. The weight loss of 23.76% was mainly ascribed to the evaporation of water and the weight decrease of 27.51% was attributed to the C, N removal and oxidation under higher temperature.

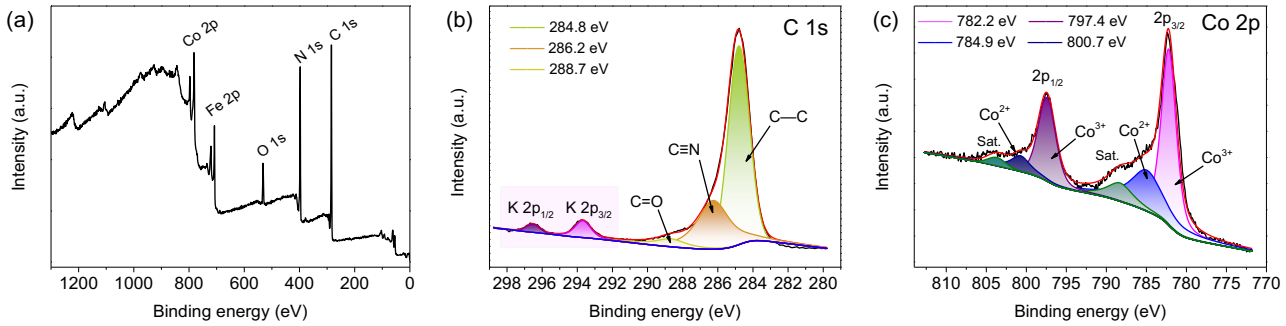

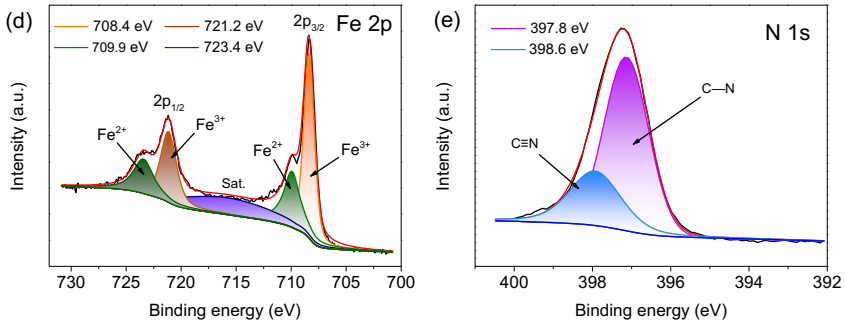

Figure S5. (a) XPS survey of the cobalt hexacyanoferrate and the corresponding high-resolution XPS spectra of (b) C 1s, (c) Co 2p, (d) Fe 2p and (e) N1s.

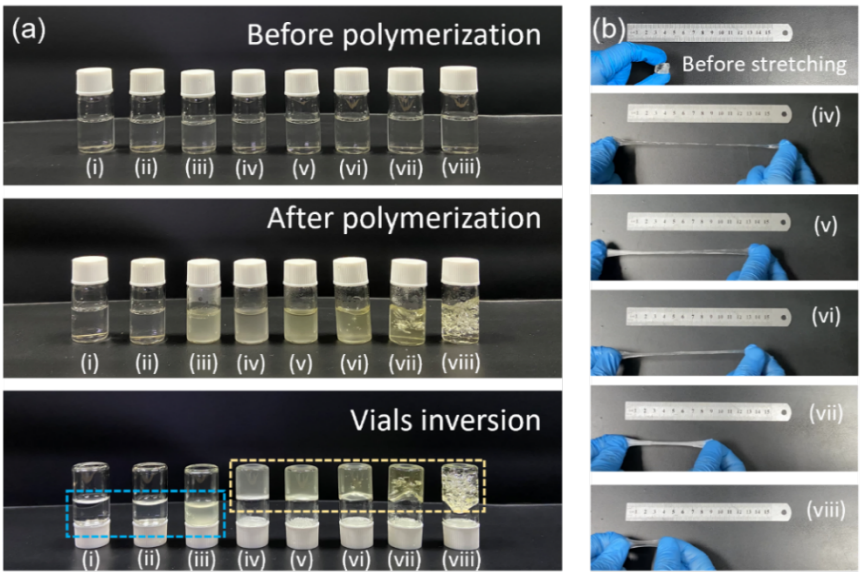

Figure S6. Optical photographs of (a) hybrid hydrogels with different mass ratios of PVA:AM monomer in 5.0 mL liquid electrolyte: (i) 0 + 0 g, (ii) 0.5 + 0 g, (iii) 0.5 + 0.5 g, (iv) 0.5 + 1.0 g, (v) 0.5 + 1.5 g, (vi) 0.5 + 2.0 g, (vii) 0.5 + 2.5 g, (viii) 0.5 + 3.0 g. (b) The corresponding stretching performance of the hydrogel with the initial size of 1.0 cm × 1.0 cm × 0.2 cm.

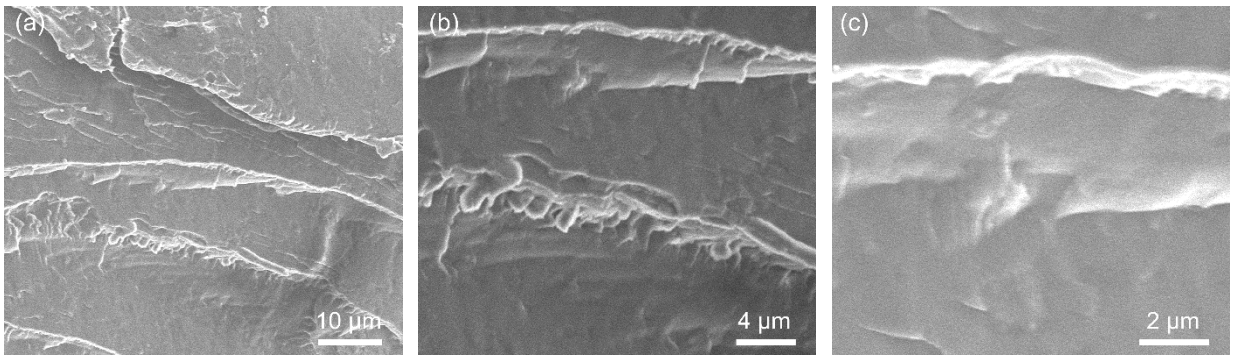

Figure S7. SEM images of freeze-dried hydrogel with 0.5 g PVA + 3.0 g AM in 5.0 mL 1.0 M $Zn(CH_3COO)_2$ liquid electrolyte.

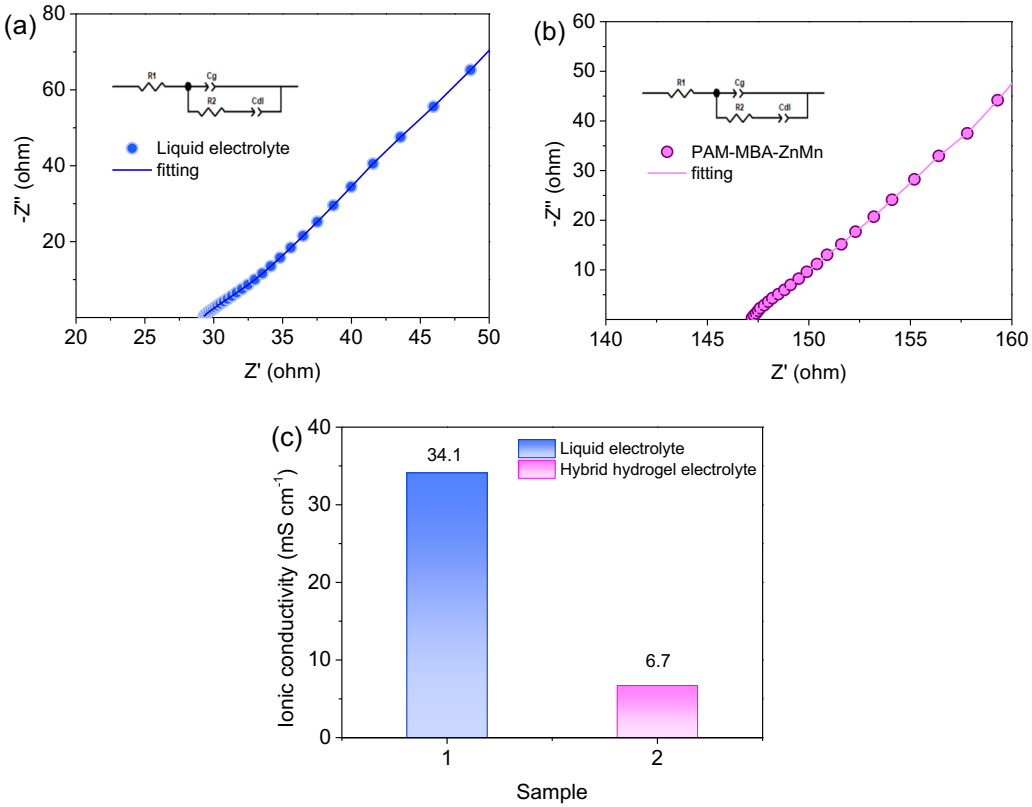

Figure S8. Nyquist plot of (a) liquid electrolyte and (b) hybrid hydrogel electrolyte. (c) Ionic conductivity.

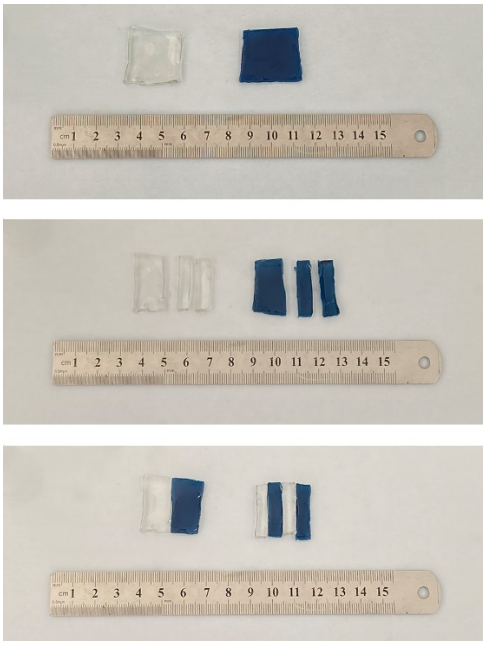

Figure S9. Self-healing performance of the as-received hybrid hydrogel electrolyte upon cutting into several pieces.

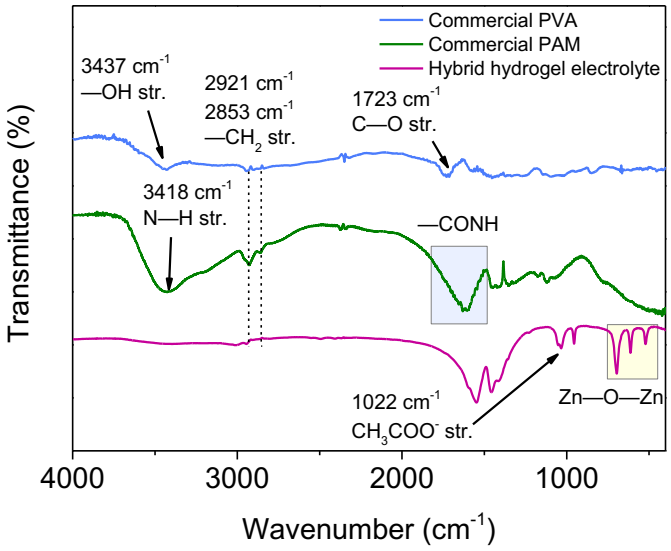

Figure S10. FI-IR spectra of commercial PAM and PVA and the hybrid hydrogel electrolyte.

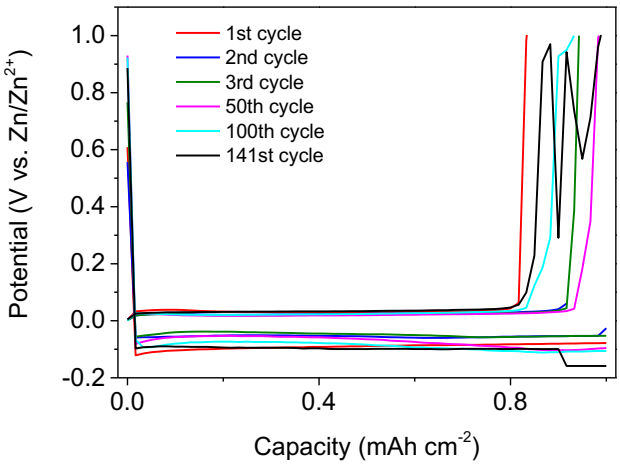

Figure S11. Polarization of liquid electrolyte in Zn||Cu asymmetric cell at 1.0 mA cm^{-2} and 1.0 mAh cm^{-2}.

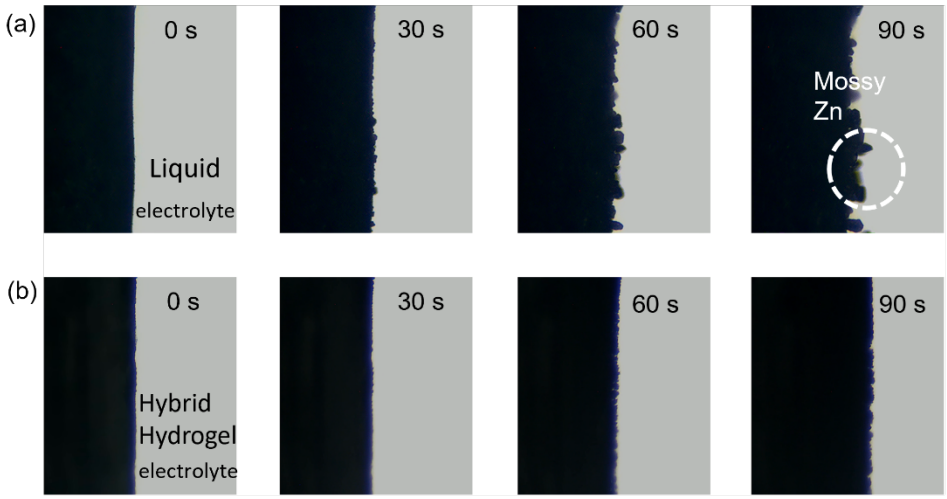

Figure S12. Operando observation of Zn deposition with (a) liquid and (b) hybrid hydrogel electrolytes under a current density of 75 mA cm^{-2}.

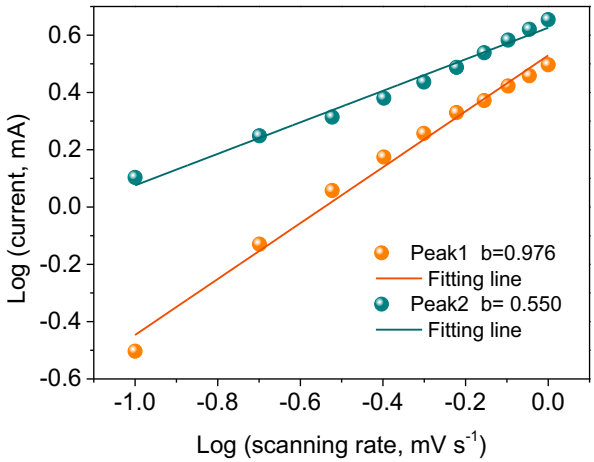

Figure S13. Plot of logarithm of peak current and scanning rate from the CV curve of the AZIB.

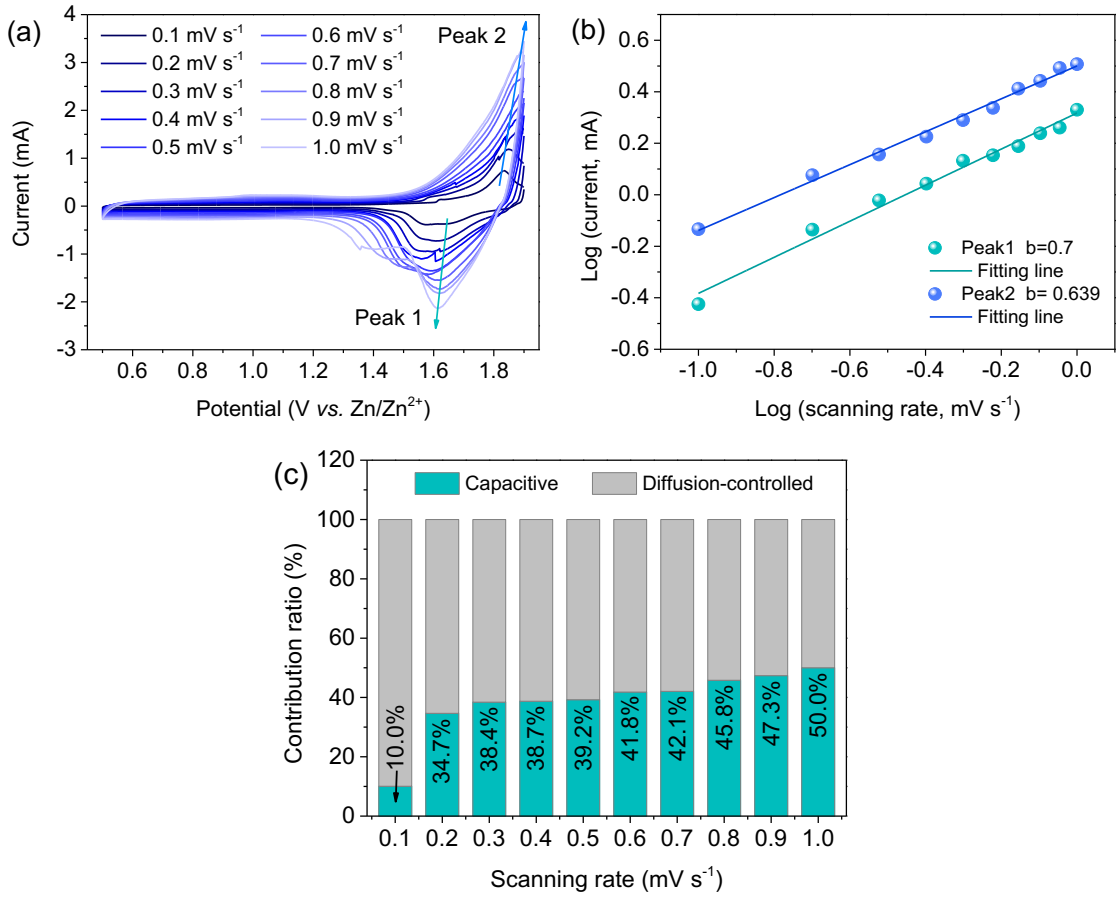

Figure S14. (a) CV curves at various scan rates of the AZIB with liquid electrolyte. (b) The corresponding logarithm of peak current and scanning rate and (c) calculated capacitive and diffusion-controlled contribution ratio.

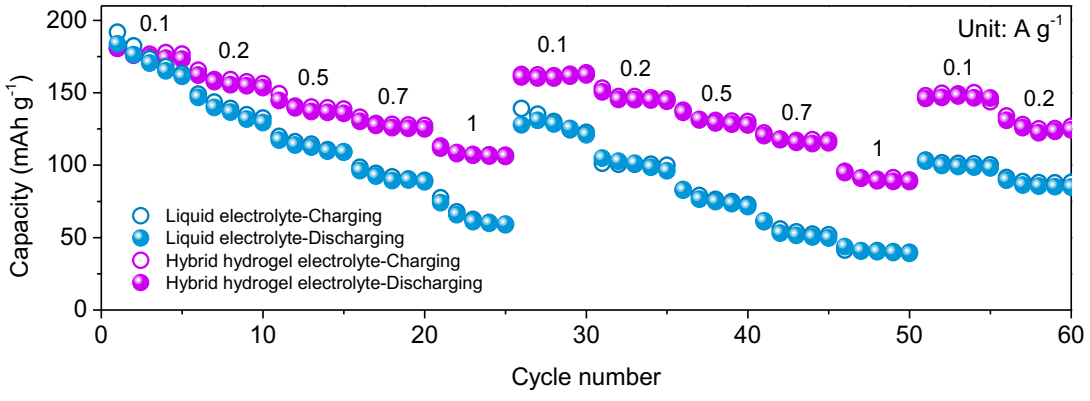

Figure S15. Rate performance of the battery at various current densities.

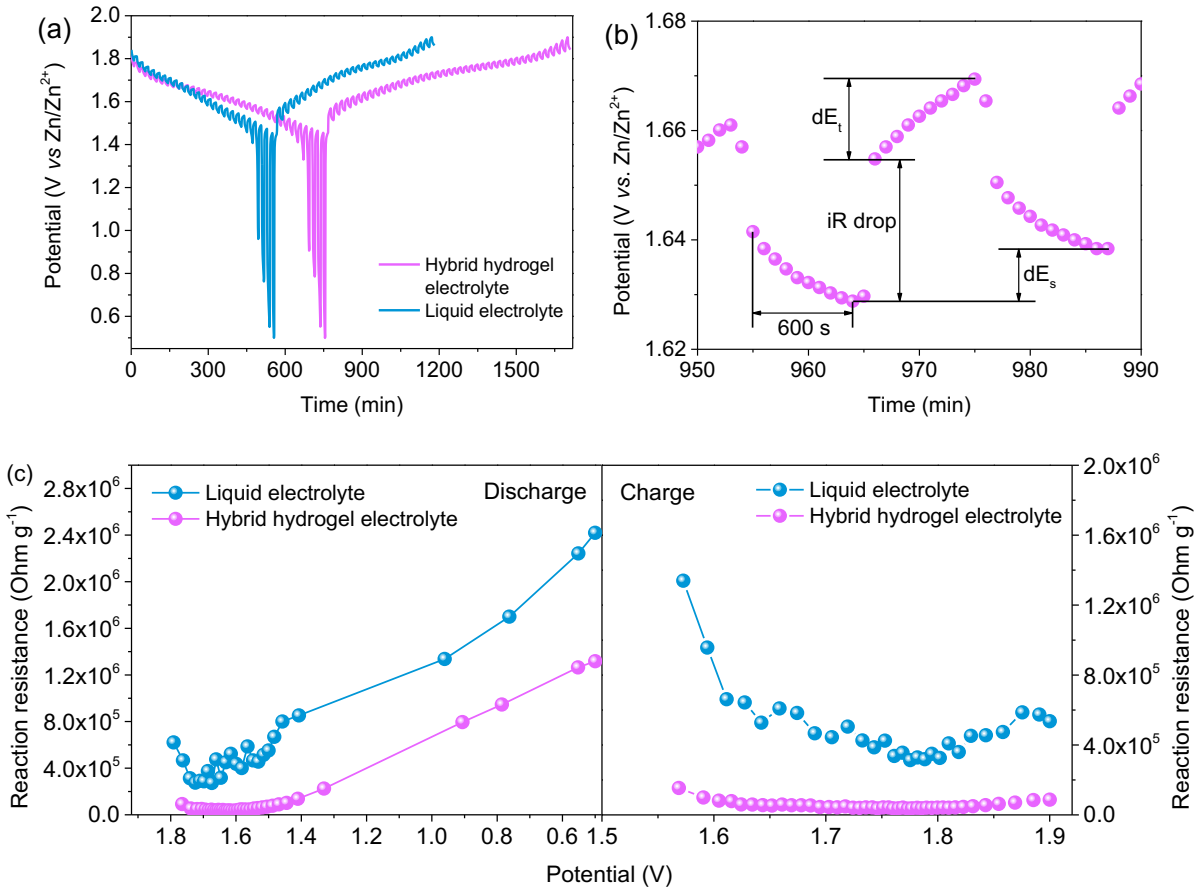

Figure S16. GITT profiles of the battery with hydrogel and liquid electrolytes. (a) Potential-time curves during the GITT measurements. (b) Illustration of dE_s, dE_t and iR drop of the battery with hydrogel electrolyte. (c) Reaction resistance of the battery under various potentials.

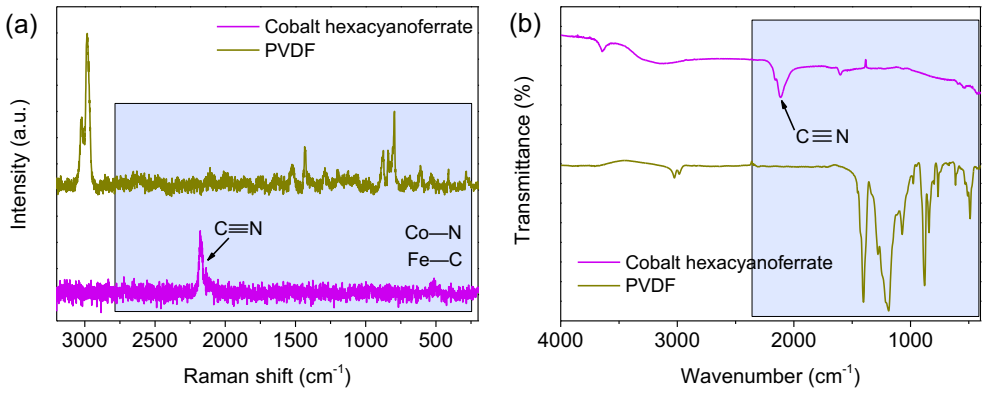

Figure S17. (a) Raman and (b) ATR-FTIR spectra of PVDF and the cobalt hexacyanoferrate.

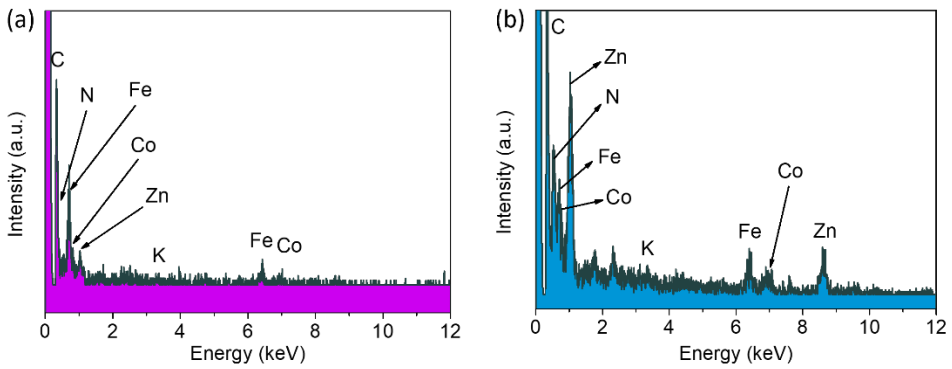

Figure S18. EDS spectra of the cobalt hexacyanoferrate NPs/CC with (a) hybrid hydrogel electrolyte and (b) liquid electrolyte after 300 cycles at 1.0 A g^{-1}.

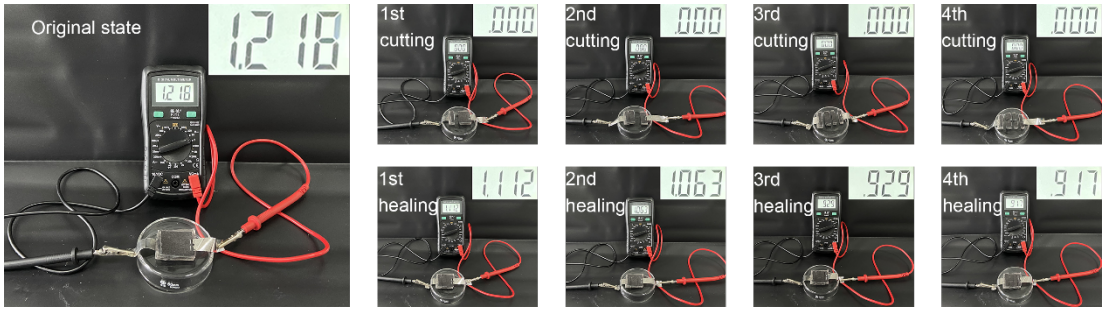

Figure S19. Battery open circuit voltage with hydrogel electrolyte after four cutting/healing cycles.

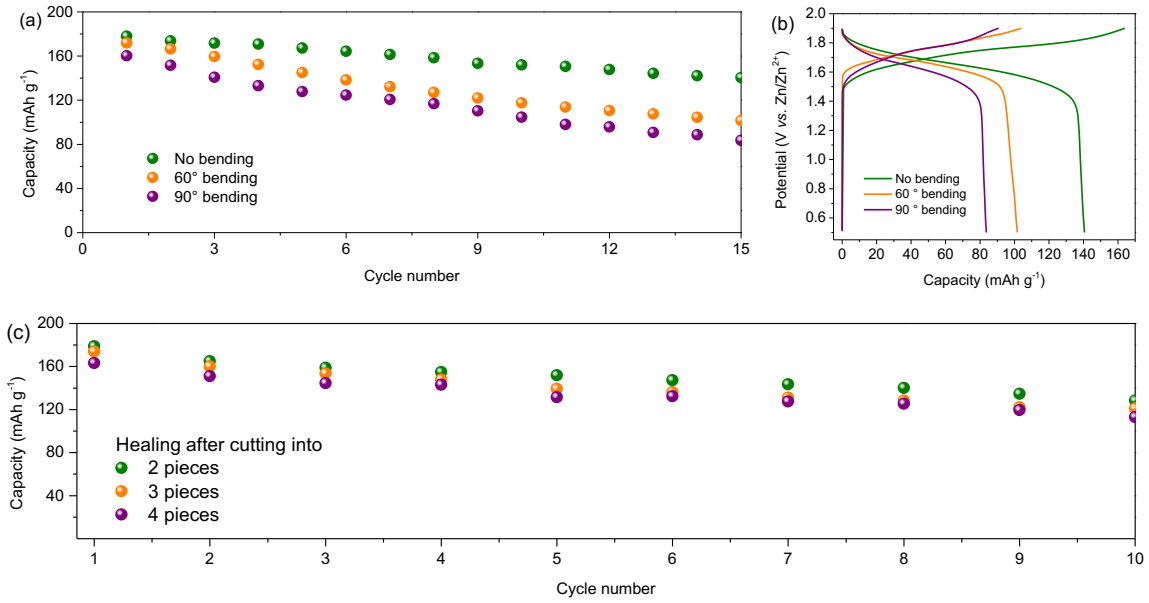

Figure S20. Flexibility and self-healing performance of the quasi-solid-state AZIBs with pure PAM hydrogel electrolyte. (a) Cycling performance and (b) GCD curves upon bending after 15 cycles. (c) Capacity retention of the battery after self-healing from cut into 2, 3 and 4 pieces.

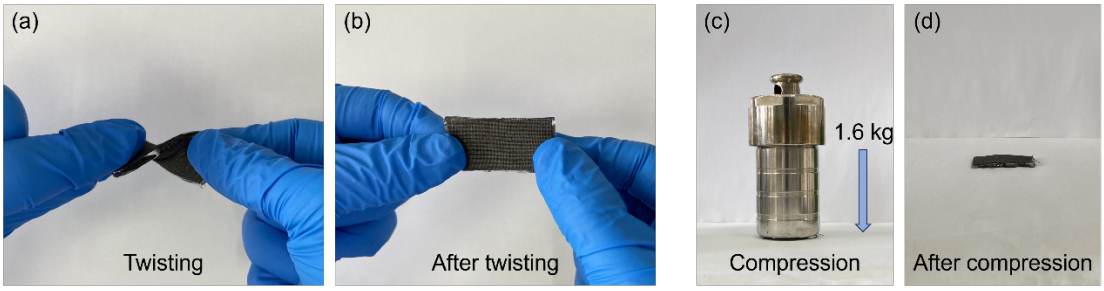

Figure S21. Flexibility of the quasi-solid-state AZIB. Upon (a) and after (b) twisting. Before (c) and after (d) compression in an autoclave.

References

1 Y. Zhang, I. Bier, V. Viswanathan, *ACS Energy Lett.*, 2022, **7**, 4061-4070.

2 Y. Shi, N. Yang, J. Niu, S. Yang, F. Wang, *Adv. Sci.*, 2022, **9**, 2200553.

3 H. Zhu, Q. Liu, S. Cao, H. Chen, Y. Liu, *Small*, 2023, DOI: 10.1002/smll.202308136.

4 Y. Qin, H. Zhao, M. Hua, J. Gao, J. Lu, S. Zhang, X. Lin, J. Sun, L. Yin, R. Wang, *J. Power Sources*, 2023, **588**, 233722.

5 Y. Jiang, C. Yang, Y. Yu, Y. Zhou, Z. Shang, S. Zhang, P. Liu, J. Zhu, M. Jiang, *J. Mater. Chem. A*, 2024, **12**, 364-374.

6 I. McClelland, S. G. Booth, N. N. Anthonisamy, L. A. Middlemiss, G. E. Pérez, E. J. Cussen, P. J. Baker, S. A. Cussen, *Chem. Mater.*, 2023, **35**, 4149-4158.

7 K. Lin, Q. Liu, Y. Zhou, H. Chen, J. Liu, J. Zhao, X. Hou, *Chem. Eng. J.*, 2023, **463**, 142464.